Available online at www.sciencedirect.com
ScienceDirect
Journal of Photochemistry and Photobiology A: Chemistry 182 (2006) 231–237
Journal of Photochemistry and Photobiology A:Chemistry
www.elsevier.com/locate/jphotochem

Stochasticity of photophysical processes in nanosystems

A.V. Barzykin, M. Tachiya*

National Institute of Advanced Industrial Science and Technology (AIST), Tsukuba, Ibaraki 305-8565, Japan

Available online 3 May 2006

Abstract

Photophysical processes in nanosystems exhibit interesting dynamics quite different from those in the bulk. Besides the cage effect, occupancy statistics of excitations becomes important. Since only a few excitations are typically present per nanosystem, bulk description of the kinetics in terms of average densities is inappropriate and one has to deal with the evolution of a discrete distribution of excitations. Here we apply this kind of stochastic approach to the description of charge carrier dynamics in isolated single-walled carbon nanotubes and singlet–triplet exciton dynamics in conjugated polymers.

Keywords: Single-walled carbon nanotubes; Conjugated polymers; Excitons; Auger recombination; Auger ionization; Triplet–triplet annihilation

1. Introduction

Modern technology has enabled one to organize, control and monitor photochemical reactions on a single molecule level. In order to enhance the performance of selected reaction channels, molecular systems are often designed in such a way that reactants are located in a close vicinity to each other, in a kind of a nanoreactor, in a very general sense. An important implication of this approach, as far as the reaction kinetics is concerned, is not just the proximity effect but also that the average number of reactants per nanosystem is small and comparable to a fluctuation. Therefore, bulk description of the kinetics in terms of average densities is inappropriate and one has to deal with the evolution of a discrete statistical distribution of reactants. A general stochastic formulation for this type of microheterogeneous kinetics has been developed in 1960s [1] and has proven itself successful at describing photodynamics in a variety of systems [2]. In this paper, we focus on our recent results including charge carrier dynamics in isolated single-walled carbon nanotubes and singlet–triplet exciton dynamics in conjugated polymers. Both systems require no special introduction due to their vast potential applications.

After the discovery of band-gap fluorescence from individual semiconducting single-walled nanotubes (SWNT) [3], much effort has been devoted to measurements of carrier dynamics after excitation [4–11]. The observed emission is dominated by excitonic recombination. Strongly bound excitons are created due to spatial confinement in the SWNT which leads to significant enhancement in the Coulombic coupling between the photoexcited electrons and holes [12–14]. Time-resolved studies have shown [4–11] that the fluorescence decay from the fundamental band edge takes place on a time scale of ∼10 ps when the excitation intensity is low (at most one electron–hole pair per nanotube is excited). This decay is mainly due to a non-radiative relaxation, identified as trapping at defects. The radiative lifetime is much longer, ∼100 ns, as estimated from the absolute fluorescence quantum efficiency [8]. A rapid decay component on a time scale of ∼1 ps emerges at elevated excitation densities as a result of exciton annihilation [9–11], most likely via the Auger mechanism [9]. Analysis of the decay kinetics on the basis of the bulk bimolecular reaction theory allowed to rule out one-dimensional diffusion of excitons as a limiting step of their annihilation [10]. A stochastic model has been suggested which takes into account the quantized character of the number of excitations in a given nanotube [9]. We will discuss this model in detail and consider implications of different physically reasonable mechanisms of Auger recombination.

Photodynamics of multichromophoric conjugated polymers (CP) has also been under recent active investigation [15–19]. Isolated CP molecules are known to behave as multichromophoric systems due to a distribution of conjugated segments on the polymer chain. Each chromophore can be either in the ground state, the singlet excitonic state, or the triplet excitonic state. The peculiar fluorescence kinetics observed in photoexcited CPs is

* Corresponding author. Tel.: +81 29 861 4412; fax: +81 29 861 6201.
E-mail address: m.tachiya@aist.go.jp (M. Tachiya).

1010-6030/$ – see front matter © 2006 Elsevier B.V. All rights reserved.
doi:10.1016/j.jphotochem.2006.03.030

understood in terms of singlet–triplet exciton interactions. While much is known about singlet excitons and the characteristic time scales of their reaction pathways, the information about triplet excitons has been difficult to obtain. The reason is in their non-emissive nature and lifetime orders of magnitude longer than that of singlets, which opens up additional relaxation channels, such as triplet–triplet annihilation and quenching by impurities. In a series of recent papers, Barbara et al. [19–22] have demonstrated the advantages of single molecule spectroscopy for the investigation of the triplet photodynamics in CPs. This technique can greatly minimize spectral and kinetic heterogeneity. The triplet dynamics is measured indirectly, by monitoring the relaxation of singlet fluorescence towards equilibrium on a time scale much longer than the singlet radiative lifetime, in response to a wide rectangular laser pulse of about 0.5 ms duration. In order to quantify experimental observations, a multi-state kinetic model has been suggested. It will be discussed in detail below. Although physically different, this model is based on essentially the same stochastic framework as the model for charge carrier dynamics in SWNTs.

2. Stochastic models of carrier dynamics in SWNT

Excited electron–hole population in an isolated nanotube decays along two main channels: by trapping at defects with the rate constant γ and by Auger recombination with the rate constant γ_A. Contribution of the radiative decay is negligible. Schematically [9]:

$$E_n \xrightarrow{n\gamma} E_{n-1}, \tag{1}$$

$$E_n \xrightarrow{(1/2)n(n-1)\gamma_A} E_{n-1}, \tag{2}$$

where E_n stands for a nanotube with n excitons. Auger recombination involves the annihilation of an electron–hole pair with the released energy transferred to the electron (or hole) of another pair. Eq. (2) assumes that this energy rapidly dissipates while the excited carrier relaxes back to the fundamental band edge. The time-dependent probability density $\rho_n(t)$ of finding n electron–hole pairs in a nanotube at time t obeys the following master equation:

$$\frac{\mathrm{d}}{\mathrm{d}t}\rho_n(t) = -\left(\gamma + \frac{1}{2}(n-1)\gamma_A\right) n\rho_n(t) + \left(\gamma + \frac{1}{2}n\gamma_A\right)(n+1)\rho_{n+1}(t). \tag{3}$$

Experimentally observable fluorescence emission rate as a function of time is proportional to the average number of excitons per nanotube:

$$\bar{n}(t) = \sum_{n=1}^{\infty} n\rho_n(t). \tag{4}$$

Let us consider first the evolution of the number of excitons in a single nanotube with n_0 excitons initially. Exact solution for this case is presented elsewhere [23]. Here we only note that the long-time fluorescence decay is governed by γ. When the "bimolecular" recombination stage is over, the remaining single electron–hole pair decays via the first-order channel, $n(t) \to n_\infty \exp(-\gamma t)$. The amplitude of the long-time tail, n_∞, is close to unity for positive n_0, since γ is typically $\ll \gamma_A$.

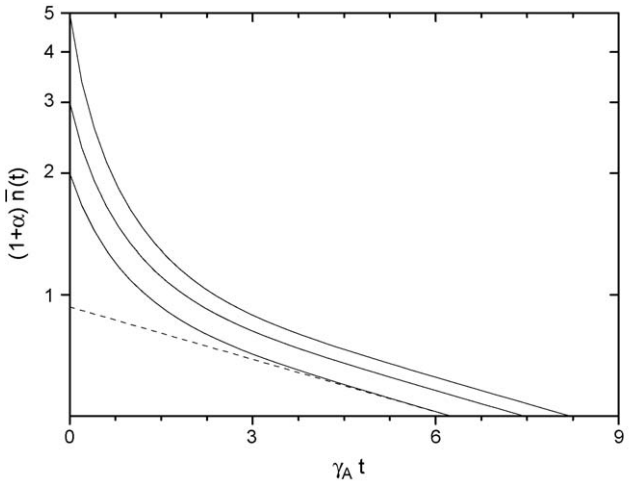

Fig. 1. Universal plot of the decay in the average number of excitons per nanotube, $(1+\alpha)\bar{n}(t)$, for the Poissonian initial distribution with $(1+\alpha)\bar{n}_0 = 2$, 3, 5 (from bottom to top) and $\gamma/\gamma_A = 0.1$, according to Eq. (13). Dashed line shows the long-time decay with the rate γ for $(1+\alpha)\bar{n}_0 = 2$. Log-linear plot.

In ordinary experimental conditions, the initial distribution of excitations in the nanotube ensemble is assumed to be Poissonian:

$$\rho_n(0) = \frac{\bar{n}_0^n}{n!}\exp(-\bar{n}_0), \tag{5}$$

with a mean occupancy number $\bar{n}_0 = \bar{n}(0) = \sigma\phi$, the product of the nanotube absorption cross-section at the pump wavelength and the number of photons per unit area in a pump pulse. The solution to Eq. (3) for the initial condition (5) can be obtained by using the generating function technique [23]. The result is

$$\frac{\bar{n}_{AR}(t)}{\bar{n}_0} = f(\bar{n}_0, t) \equiv \sum_{i=1}^{\infty}(z+2i-1)\,\bar{n}_0^{i-1} \times \exp\left[-\bar{n}_0 - \frac{1}{2}\gamma_A i(i+z-1)t\right] \times \sum_{j=0}^{\infty}\frac{\bar{n}_0^j}{j!}\frac{\Gamma(z+i+j)}{\Gamma(z+2i+j)}, \tag{6}$$

where $z = 2\gamma/\gamma_A$. Eq. (6) predicts a multiexponential decay, as it was indeed observed experimentally. See Fig. 1 in Ref. [9] where experimental data were fit by a numerical solution of Eq. (3). The long-time decay rate is γ, as expected. The corresponding amplitude is given by

$$\bar{n}_\infty = \bar{n}_0 g(\bar{n}_0) \equiv \bar{n}_0 \mathrm{e}^{-\bar{n}_0}\sum_{j=0}^{\infty}\frac{\bar{n}_0^j}{j!}\frac{1+z}{j+1+z}. \tag{7}$$

It increases linearly with $\bar{n}_0$, which is proportional to the excitation density, when excitation density is low but then saturates and tends to $1+z$ for large $\bar{n}_0$. $1+z$ is a kinetic factor reflecting the competition between exciton annihilation and first-order relaxation. This behavior was observed experimen-

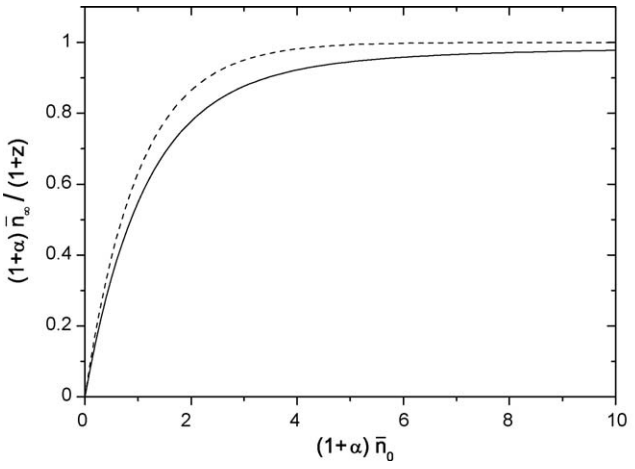

Fig. 2. Universal plot of the normalized amplitude of the long-time decay, $(1+\alpha)\bar{n}_\infty/(1+z)$, as a function of the initial average number of excitons per nanotube, $(1+\alpha)\bar{n}_0$, for Poissonian initial condition and $\gamma/\gamma_A = 0.1$. Solid line illustrates Eq. (14), dashed line corresponds to the limit of $\gamma = 0$ where $(1+\alpha)\bar{n}_\infty = 1 - \exp(-(1+\alpha)\bar{n}_0)$.

tally (see Fig. 2 in Ref. [9]). In the limit of $\gamma = 0$ ($z = 0$) we have at long times, $\bar{n}_\infty = 1 - \exp(-\bar{n}_0)$. This simple formula describes the saturation behavior quite well, since $\gamma \ll \gamma_A$ in experiment ($\gamma/\gamma_A = 0.1$ was obtained in Ref. [9]). Illustrations will be presented below.

In nanoparticles, Auger recombination may occur with the ejection of the electron (or hole) of another pair to the surrounding matrix (Auger ionization) [24,25]. Effectively, two excitons disappear as a result of annihilation:

$$E_n \xrightarrow{(1/2)n(n-1)\gamma_A} E_{n-2}. \tag{8}$$

Strong carrier confinement in SWNT suggests that the ejection effect may be important there as well. In nanoparticles, charge-separated electron–hole pair becomes an efficient excitation quencher, responsible for the blinking phenomenon [25]. Whether this is also relevant to SWNT is not clear, although blinking was indeed observed in SWNT at room temperature [26]. For the time being let us consider a hypothetical situation where the charge-separated pair quenches the remaining excitations infinitely fast, so that the Auger process effectively leads to disappearance of all excitons in a given nanotube, $E_n \to E_0$. The amplitude of the long-time tail of the fluorescence decay can be estimated by neglecting the first-order relaxation. It is given by $\bar{n}_\infty = \bar{n}_0 \exp(-\bar{n}_0)$, the fraction of nanotubes with one exciton initially. No saturation is predicted, in contrast to experimental observations, but rather a decrease of $\bar{n}_\infty$ for high excitation densities. Therefore, we may conclude that the charge-separated pairs, if they exist at all, may not be effective quenchers of other excitations on the time scale of experiment. We consider a phenomenological model where only the processes (1) and (8) are involved. The master equation transforms into:

$$\frac{\mathrm{d}}{\mathrm{d}t}\rho_n(t) = -\left(\gamma + \frac{1}{2}(n-1)\gamma_A\right) n\rho_n(t) + (n+1)\gamma\rho_{n+1}(t) + \frac{1}{2}(n+1)(n+2)\gamma_A\rho_{n+2}(t). \tag{9}$$

Let us again consider the evolution of the number of excitons in a single nanotube with n_0 excitons initially. In contrast to the Auger recombination model, the decay is different for even and odd n_0. For example, in a special situation where the first-order relaxation rate is negligible ($\gamma = 0$), the number of surviving excitons at long times is zero for even n_0 and 1 for odd n_0, i.e., $n_\infty = (1/2)[1 - (-1)^{n_0}]$. However, experimentally significant is the decay from the Poissonian initial distribution. Interestingly, exact solution to Eq. (9) with the initial condition of Eq. (5) coincides with Eq. (6) except for a "scaling" factor of 2 for the average number of excitons [23]:

$$\frac{\bar{n}_{AI}(t)}{\bar{n}_0} = f(2\bar{n}_0, t). \tag{10}$$

Since the nanotube absorption cross-section σ (and thus $\bar{n}_0 = \sigma\phi$) is an adjustable parameter in experiments of Wang et al. [9] and fluorescence emission is measured in relative, rather than absolute, units, we must conclude that the two models were *indistinguishable* in those experiments. In order to prove or disprove the Auger ionization mechanism on the basis of kinetic measurements, the nanotube absorption cross-section has to be accurately determined, as it was done for nanoparticles [27]. Recent observation of the photoluminescence intermittency in individual SWNT suggests that the Auger ionization is a reasonable possibility.

The observed intermittency in nanotubes was individual nanotube selective, i.e., only some SWNTs showed intermittency while most of them did not [26]. This leads us to suggest that both Auger recombination and ionization may occur at the same time. Schematically:

$$E_n \xrightarrow{(1/2)n(n-1)\gamma_A(1-\alpha)} E_{n-1}, \tag{11}$$

$$E_n \xrightarrow{(1/2)n(n-1)\gamma_A\alpha} E_{n-2}, \tag{12}$$

where α denotes the relative contribution of Auger ionization and varies from 0 to 1. The master equation corresponding to Eqs. (1), (11), (12) can be written in a similar way to Eqs. (3) and (9). It can be solved exactly via a transformation to a partial differential equation by using the generating function, as it was done in Ref. [23]. Here we only present the result for the Poissonian initial condition:

$$\frac{\bar{n}_{MA}(t)}{\bar{n}_0} = f[\bar{n}_0(1+\alpha), t], \tag{13}$$

where the function $f(\bar{n}_0, t)$ is defined by Eq. (6). The amplitude of the long-time decay is given by

$$\frac{\bar{n}_\infty}{\bar{n}_0} = g[\bar{n}_0(1+\alpha)], \tag{14}$$

where the function $g(\bar{n}_0)$ is defined by Eq. (7). What we have obtained is a general "scaling" relationship for the mixed Auger mechanism in terms of the average number of excitons. The original Auger recombination result is reproduced for $\alpha = 0$, while $\alpha = 1$ corresponds to the Auger ionization model. We note again that the two mechanisms were indistinguishable in experiments so far raising an interesting challenge for future studies.

Fig. 1 illustrates the universal decay kinetics for different excitation intensities, according to Eq. (13). These kinetics have been observed experimentally by Wang et al. (see Fig. 1 in Ref. [9]). Fig. 2 illustrates saturation of the amplitude of the long-time decay as a function of excitation intensity, in agreement with experimental observations (see Fig. 2 in Ref. [9]).

3. Stochastic models of photodynamics in CP

As mentioned in Section 1, isolated CP molecules behave as multichromophoric systems. For example, there are ∼50 effective chromophores for the F8BT molecules, poly(9,9′-dioctylfluorene cobenzothiadiazole). The population state of a whole CP molecule corresponds to each chromophore occupying either the ground state, the singlet excitonic state, or the triplet excitonic state at a given time. It is assumed that only the numbers of each type of electronic state define the population state, not their specific configuration in the polymer chain [20]. This assumption implies locally homogeneous kinetics and a narrow distribution of site energies. The number of excitons continuously and spontaneously fluctuates. These fluctuations are well described by a set of first-order incoherent rate processes, which govern transitions between population states of the CP molecule. Since the time scale of singlet decay is orders of magnitude faster than that of triplet decay, we can separate the kinetics of triplet decay from that of singlet decay. The kinetics of triplet decay is described in terms of the number n of triplet excitons in the polymer chain, which is denoted by CP_n. The kinetic scheme is given by [28]:

$$\mathrm{CP}_n \xrightarrow{k_{\mathrm{f},n}} \mathrm{CP}_{n+1}, \tag{15}$$

$$\mathrm{CP}_n \xrightarrow{nk_{\mathrm{b}}} \mathrm{CP}_{n-1}, \tag{16}$$

$$\mathrm{CP}_n \xrightarrow{(1/2)n(n-1)k_{\mathrm{tt}}} \mathrm{CP}_{n-2}. \tag{17}$$

Here $k_{\mathrm{f},n}$ stands for the effective rate constant of triplet formation in a CP already containing n triplets:

$$k_{\mathrm{f},n} = \frac{k_{\mathrm{exc}}k_{\mathrm{isc}}\tau_{\mathrm{fl}}}{1 + k_{\mathrm{isc}}\tau_{\mathrm{fl}} + nk_{\mathrm{q}}\tau_{\mathrm{fl}}} \simeq \frac{k_{\mathrm{exc}}k_{\mathrm{isc}}\tau_{\mathrm{fl}}}{1 + nk_{\mathrm{q}}\tau_{\mathrm{fl}}}, \tag{18}$$

where $k_{\mathrm{exc}} = I_{\mathrm{exc}}\sigma$ is the excitation rate, k_{isc} the intersystem crossing (ISC) rate, k_{q} the singlet quenching rate by triplets, τ_{fl} the singlet fluorescence lifetime, I_{exc} the incident excitation intensity, and σ is the absorption cross-section of the polymer molecule. Eq. (18) implies that triplet formation proceeds through singlet excitation followed by ISC which competes with radiative decay and quenching. The rate of back reaction, Eq. (16), is governed by reverse ISC, $k_{\mathrm{b}} = k'_{\mathrm{isc}}$. k_{tt} is the first-order rate constant of triplet–triplet annihilation in a CP molecule with two triplets.

The above kinetic scheme corresponds to the following set of rate equations for the probability $P_n(t)$ to find n triplets in a CP molecule at time t:

$$\frac{\mathrm{d}}{\mathrm{d}t}P_n(t) = k_{\mathrm{f},n-1}P_{n-1}(t) - \left[k_{\mathrm{f},n} + nk_{\mathrm{b}} + \frac{1}{2}n(n-1)k_{\mathrm{tt}}\right]P_n(t) + k_{\mathrm{b}}(n+1)P_{n+1}(t) + \frac{1}{2}(n+1)(n+2)k_{\mathrm{tt}}P_{n+2}(t). \tag{19}$$

In a typical experiment, one irradiates a single CP molecule with a repetitive sequence of rectangular excitation pulses of about 0.5 ms each [21]. The pulse duration is chosen to be long enough so that the stationary stage is reached in the emission transient. Therefore, one can consider the kinetics under the condition of continuous irradiation, with the initial condition for Eq. (19) given by $P_n(0) = \delta_{n,0}$, where δ is the Kronecker delta. The quantity experimentally observed is the fluorescence intensity due to singlet excitons. If a CP molecule contains n triplets, the quantum yield of fluorescence is given by $1/(1 + nk_{\mathrm{q}}\tau_{\mathrm{fl}})$. Therefore, the emission yield is given by

$$I(t) = I(0)\sum_{n=0}^{\infty}\frac{P_n(t)}{1 + nk_{\mathrm{q}}\tau_{\mathrm{fl}}}, \tag{20}$$

where $I(0)$ is the emission intensity right after the laser pulse is turned on. The observed fluorescence intensity decays with time as the number of triplets in a CP molecule increases. At long times, the stationary stage is reached about the distribution of triplets.

Eq. (19) cannot be solved analytically. Numerical analysis will be presented below. A useful analytical result can be obtained, however, under the assumption of infinitely fast triplet–triplet annihilation. In this limit, a given CP molecule will contain only zero or one triplet exciton. This corresponds to a two-state model of Barbara et al. [21], which predicts the following exponential relaxation kinetics:

$$\frac{I(t)}{I(0)} = \frac{I(\infty)}{I(0)} + \left[1 - \frac{I(\infty)}{I(0)}\right]\exp(-k_{\infty}t), \tag{21}$$

where

$$k_{\infty} = k_{\mathrm{f},0} + k_{\mathrm{b}} + k_{\mathrm{f},1}, \tag{22}$$

and $I(\infty)/I(0)$ is related to the so-called contrast ratio and expressed in terms of the model parameters [28]. The meaning of Eq. (22) is simple: k_{∞} is a sum of the forward, $k_{\mathrm{f},0}$, and backward, $k_{\mathrm{b}} + k_{\mathrm{f},1}$, rates of the reversible reaction between two states, CP_0 and CP_1. The back reaction is supplemented by an additional channel, the disappearance of the triplet already present in the CP molecule by triplet–triplet annihilation with a newly formed triplet. Since triplet–triplet annihilation is assumed to be infinitely fast, the rate of the additional channel is given by the rate of formation of a new triplet, $k_{\mathrm{f},1}$. We have already compared the two-state model versus the multi-state model of exciton dynamics and found reasonable agreement for low excitation intensity and fast triplet–triplet annihilation rate, as expected [28]. The two-state model fails when either of these conditions is not fulfilled. The stationary fluorescence intensity turns out to be the most sensitive parameter.

In order to illustrate the predictions of the multi-state stochastic model, we choose a typical set of parameter values cor-

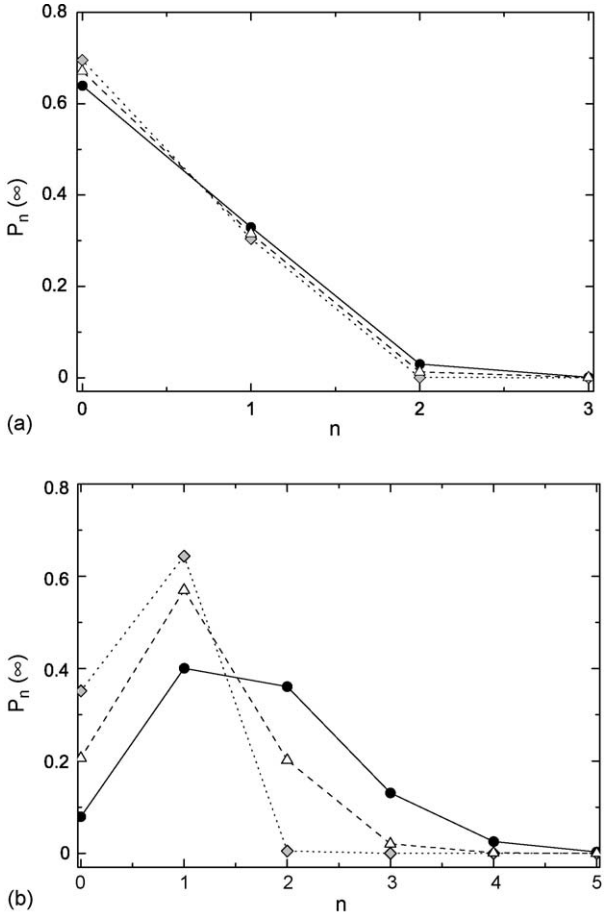

Fig. 3. Stationary distribution of triplets in a CP molecule at low ($k_f^0/k'_{isc} = 0.52$ (a)) and high ($k_f^0/k'_{isc} = 5.2$ (b)) excitation intensity for slow ($k_{tt}/k'_{isc} = 0.025$, circles), intermediate ($k_{tt}/k'_{isc} = 2.5$, triangles), and fast ($k_{tt}/k'_{isc} = 250$, diamonds) triplet–triplet annihilation. Other parameters were chosen to represent the F8BT molecule, as specified in the text.

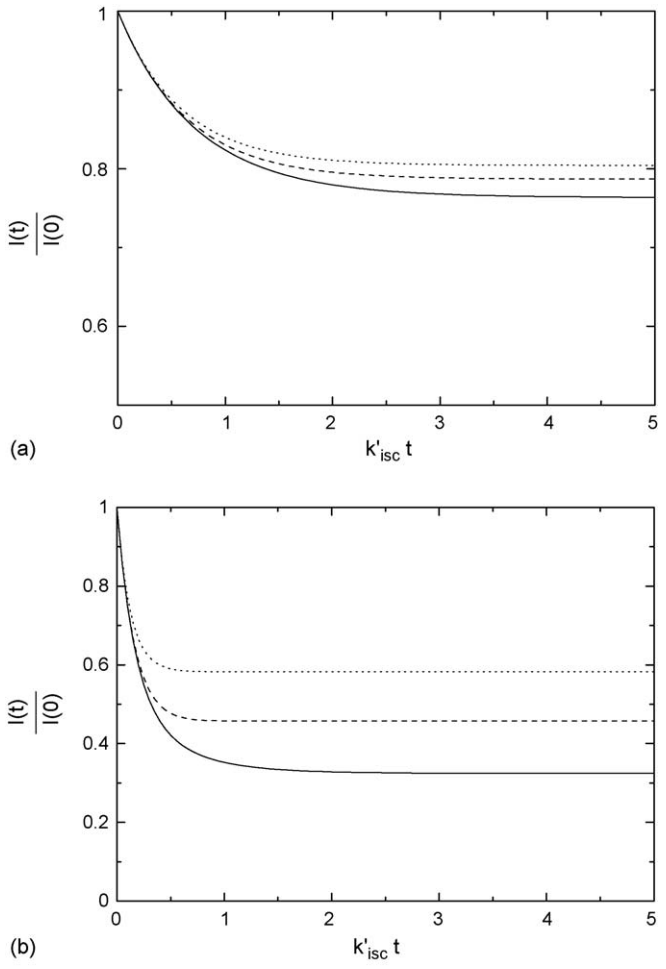

Fig. 4. Fluorescence relaxation kinetics at low ($k_f^0/k'_{isc} = 0.52$ (a)) and high ($k_f^0/k'_{isc} = 5.2$ (b)) excitation intensity for slow ($k_{tt}/k'_{isc} = 0.025$, solid), intermediate ($k_{tt}/k'_{isc} = 2.5$, dashed), and fast ($k_{tt}/k'_{isc} = 250$, dotted) triplet–triplet annihilation. Other parameters were chosen to represent the F8BT molecule, as specified in the text.

responding to one of the CP molecules studied by Barbara et al., namely, the F8BT molecule [21]. Thus we set $k_{isc} = 7 \times 10^6\,s^{-1}$, $k'_{isc} = 2 \times 10^3\,s^{-1}$, $k_q = 6 \times 10^8\,s^{-1}$, and $\tau_{fl} = 3 \times 10^{-9}$ s. We consider three limits of triplet–triplet annihilation: fast ($k_{tt} \gg k'_{isc}$), intermediate ($k_{tt} \sim k'_{isc}$), and slow ($k_{tt} \ll k'_{isc}$). In the fast annihilation limit, the kinetics is saturated with respect to k_{tt} in a sense that any further increase in k_{tt} beyond the chosen value of $k_{tt}/k'_{isc} = 250$ does not lead to any significant change in the fluorescence relaxation kinetics. As regards the excitation intensity, we consider relatively high and low limits here as well. We define the excitation intensity via a dimensionless parameter $k_f^0/k'_{isc} = k_{exc}k_{isc}\tau_{fl}/k'_{isc}$, proportional to I_{exc}. Whether the excitation intensity is high or low for a given set of other parameters can be judged by the value of $I(\infty)/I(0)$. The low excitation intensity limit corresponds to $I(\infty)/I(0) \simeq 0.8$. Lower intensities are of marginal interest. The high intensity limit corresponds to $I(\infty)/I(0) \simeq 0.5$, roughly speaking, the deepest fluorescence relaxation level observed in experiments by Barbara et al. [21].

Fig. 3 shows the stationary distribution of triplets. Recall that initially there are no triplets in the system, $P_n(0) = \delta_{n,0}$. Only a small fraction of CP molecules is occupied by two triplets when the excitation intensity is low (Fig. 3a). For high excitation intensity (Fig. 3b), multiple occupancy of a CP molecule by triplets becomes significant as triplet–triplet annihilation slows down. Fig. 4 shows the calculated fluorescence relaxation kinetics. Similar decays were observed in experiment [19–22]. For low excitation intensity (Fig. 4a), the kinetics is exponential, Eq. (21), and weakly sensitive to the triplet–triplet annihilation rate. For high excitation intensity (Fig. 4b), the effect of finite triplet–triplet annihilation rate is very important. The kinetics is non-exponential at short times but long-time approach to the stationary fluorescence level is exponential so that we can define the long-time fluorescence relaxation constant as follows:

$$k_\infty = -\frac{\mathrm{d}\,\ln[I(t) - I(\infty)]}{\mathrm{d}t}. \tag{23}$$

Fig. 5 shows the normalized stationary fluorescence intensity as a function of excitation power. Experimentally, the excitation power is chosen so that the stationary fluorescence level be at least 20% lower than the initial fluorescence level. Therefore, the effect of triplet–triplet annihilation rate is always important experimentally, as far as the stationary fluorescence intensity

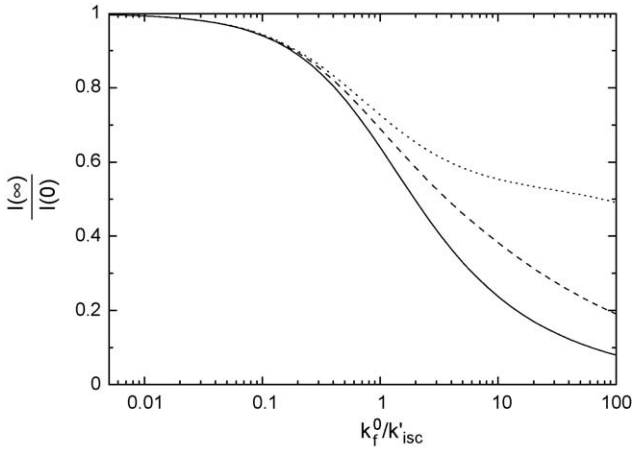

Fig. 5. Normalized stationary fluorescence intensity as a function of excitation power (via k_f^0/k'_{isc}) for slow ($k_{tt}/k'_{isc} = 0.025$, solid), intermediate ($k_{tt}/k'_{isc} = 2.5$, dashed), and fast ($k_{tt}/k'_{isc} = 250$, dotted) triplet–triplet annihilation. Other parameters were chosen to represent the F8BT molecule, as specified in the text.

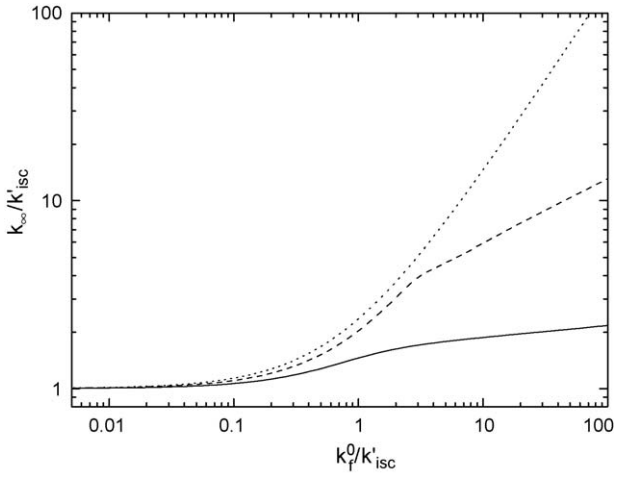

Fig. 7. Long-time fluorescence decay constant, k_∞, as a function of excitation power (via k_f^0/k'_{isc}) for slow ($k_{tt}/k'_{isc} = 0.012$, solid), intermediate ($k_{tt}/k'_{isc} = 1.2$, dashed), and fast ($k_{tt}/k'_{isc} = 1200$, dotted) triplet–triplet annihilation. Other parameters were chosen to represent the F8BT molecule, as specified in the text.

is concerned. Saturation with respect to the triplet–triplet annihilation rate is achieved only for $k_{tt}/k'_{isc} \gg 100$, as shown in Fig. 6. Fig. 7 shows that the effect of triplet–triplet annihilation rate on the long-time fluorescence relaxation constant is also quite pronounced. Eq. (22) of the two-state model predicts a linear dependence of k_∞ on the excitation intensity. This limit is reached only at very high triplet–triplet annihilation rate. However, saturation of k_∞ with respect to k_{tt} is achieved already at $k_{tt}/k'_{isc} \sim 10$, as shown in Fig. 8. The triplet–triplet annihilation rate depends on the system size and the triplet diffusion coefficient. For larger systems and/or for those systems where, for some reason, the diffusion is slow, triplet–triplet annihilation will also be slow thus making the multi-state analysis especially important.

The multi-state kinetic model can also be used to analyze fluorescence blinking resulting from 'real-time' fluctuations in the number of triplets in a single CP molecule after the laser is turned on. We have already shown [28] that the amplitude of fluctuations in the occupancy is basically determined by the triplet–triplet annihilation rate, while their frequency is sensitive to the excitation intensity. One can distinguish between zero and non-zero occupancies from the observed singlet fluorescence intensity. However, it is difficult to distinguish from the fluorescence intensity between different non-zero occupancies. In addition, fluorescence intensities from non-zero occupancies can be easily mixed up with background noise. On the other hand, the experimental technique of Barbara et al. [21], although measuring only statistically averaged singlet fluorescence, has proven to be rather sensitive to higher occupancy numbers in the distribution of triplets.

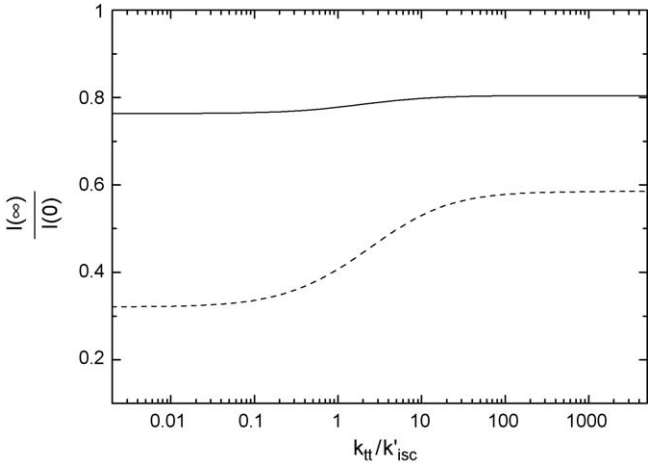

Fig. 6. Normalized stationary fluorescence intensity as a function of the triplet–triplet annihilation rate for low ($k_f^0/k'_{isc} = 0.52$, solid) and high ($k_f^0/k'_{isc} = 5.2$, dashed) excitation intensity. Other parameters were chosen to represent the F8BT molecule, as specified in the text.

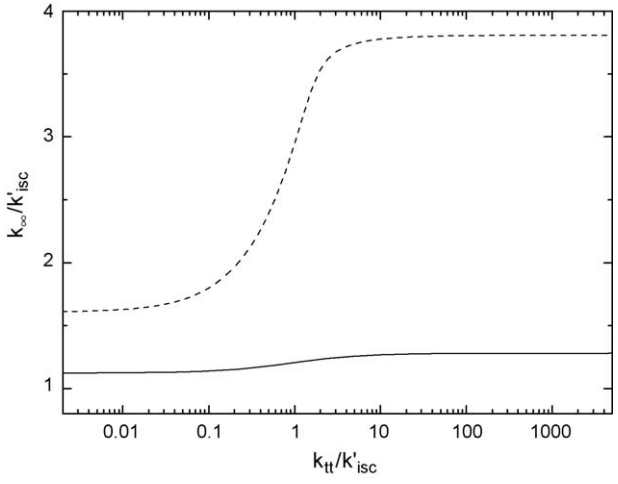

Fig. 8. Long-time fluorescence decay constant, k_∞, as a function of the triplet–triplet annihilation rate for low ($k_f^0/k'_{isc} = 0.21$, solid) and high ($k_f^0/k'_{isc} = 2.1$, dashed) excitation intensity. Other parameters were chosen to represent the F8BT molecule, as specified in the text.

4. Concluding remarks

Stochastic approach is a natural way to analyze photodynamics in nanosystems, with a limited number of excitations. In this paper, we have discussed applications of this approach to the description of charge carrier dynamics in isolated single-walled carbon nanotubes and singlet–triplet exciton dynamics in conjugated polymers. We have derived an analytical solution for the model of carrier dynamics in SWNT, originally suggested by Wang et al. Numerical analysis of this model has already shown good quantitative agreement with the measured decay data [9]. This model and the solution presented should apply equally well to nanoparticles [27]. We have also analyzed possible implications of the Auger ionization on the carrier relaxation dynamics. An interesting outcome of this analysis is a scaling relationship for the observable fluorescence emission kinetics with and without Auger ionization, in terms of the average number of excitons per nanotube. Whether it will be possible to distinguish between the two mechanisms depends on future experimental efforts. We have also presented and analyzed numerically a multi-state stochastic model of singlet–triplet exciton dynamics in CP molecules. We believe that the power of the experimental technique developed by Barbara et al. [21] for probing triplet photodynamics in CPs by measuring singlet fluorescence relaxation is not fully exploited if the data is analyzed on the basis of the two-state model, as it was done previously. The multi-state model approach should provide more accurate quantitative information on the kinetic processes involved. In particular, it allows for determination of the triplet–triplet annihilation rate which is not directly included in the two-state model.

References

[1] D.A. McQuarrie, Adv. Chem. Phys. 15 (1969) 149.
[2] M. Tachiya, in: G.R. Freeman (Ed.), Kinetics of Nonhomogeneous Processes, Wiley, New York, 1987, p. 575.
[3] M. O'Connell, S.M. Bachilo, C.B. Huffman, V.C. Moore, M.S. Strano, E.H. Haroz, K.L. Rialon, P.J. Boul, W.H. Noon, C. Kittrell, J. Ma, R.H. Hauge, R.B. Weisman, R.E. Smalley, Science 297 (2002) 593.
[4] J.-S. Lauret, C. Voisin, G. Cassabois, C. Delalande, Ph. Roussignol, O. Jost, L. Capes, Phys. Rev. Lett. 90 (2003) 057404.
[5] A. Hagen, G. Moos, V. Talalaev, T. Hertel, Appl. Phys. A 78 (2004) 1137.
[6] O.J. Korovyanko, C.-X. Sheng, Z.V. Vardeny, A.B. Dalton, R.H. Baughman, Phys. Rev. Lett. 92 (2004) 017403.
[7] G.N. Ostojic, S. Zaric, J. Kono, M.S. Strano, V.C. Moore, R.H. Hauge, R.E. Smalley, Phys. Rev. Lett. 92 (2004) 117402.
[8] F. Wang, G. Dukovic, L.E. Brus, T.F. Heinz, Phys. Rev. Lett. 92 (2004) 177401.
[9] F. Wang, G. Dukovic, E. Knoesel, L.E. Brus, T.F. Heinz, Phys. Rev. B 70 (2004) 241403(R).
[10] Y.-Z. Ma, J. Stenger, J. Zimmermann, S.M. Bachilo, R.E. Smalley, R.B. Weisman, G.R. Fleming, J. Chem. Phys. 120 (2004) 3368.
[11] Y.-Z. Ma, L. Valkunas, S.L. Dexheimer, S.M. Bachilo, G.R. Fleming, Phys. Rev. Lett. 94 (2005) 157402.
[12] T.G. Pedersen, Phys. Rev. B 67 (2003) 073401.
[13] C.L. Kane, E.J. Mele, Phys. Rev. Lett. 90 (2003) 207401.
[14] V. Perebeinos, J. Tersoff, P. Avouris, Phys. Rev. Lett. 92 (2004) 257402.
[15] J. Yu, D. Hu, P.F. Barbara, Science 289 (2000) 1327.
[16] M. Segal, M.A. Baldo, R.J. Holmes, S.R. Forrest, Z.G. Soos, Phys. Rev. B 68 (2003) 075211.
[17] A. Kadashchuk, A. Vakhnin, I. Blonski, D. Beljonne, Z. Shuai, J.L. Bredas, V.I. Arkhipov, P. Heremans, E.V. Emelianova, H. Bassler, Phys. Rev. Lett. 93 (2004) 066803.
[18] O. Mirzov, F. Cichos, C. von Borczyskowski, I.G. Scheblykin, Chem. Phys. Lett. 386 (2004) 286.
[19] P.F. Barbara, A.J. Gesquiere, S.-J. Park, Y.-J. Lee, Acc. Chem. Res. 38 (2005) 602.
[20] J. Yu, R. Lammi, A.J. Gesquiere, P.F. Barbara, J. Phys. Chem. B 109 (2005) 10025.
[21] A.J. Gesquiere, Y.J. Lee, J. Yu, P.F. Barbara, J. Phys. Chem. B 109 (2005) 12336, equations (8) and (12) in this article contain misprints.
[22] A.J. Gesquiere, S.-J. Park, P.F. Barbara, J. Am. Chem. Soc. 127 (2005) 9556.
[23] A.V. Barzykin, M. Tachiya, Phys. Rev. B 72 (2005) 075425.
[24] D.I. Chepic, A.L. Efros, A.I. Ekimov, M.G. Ivanov, V.A. Kharchenko, I.A. Kudriavtsev, T.V. Yazeva, J. Lumin. 47 (1990) 113.
[25] A.L. Efros, M. Rosen, Phys. Rev. Lett. 78 (1997) 1110.
[26] K. Matsuda, Y. Kanemitsu, K. Irie, T. Saiki, T. Someya, Y. Miyauchi, S. Maruyama, Appl. Phys. Lett. 86 (2005) 123116.
[27] V.I. Klimov, A.A. Mikhailovsky, D.W. McBranch, C.A. Leatherdale, M.G. Bawendi, Science 287 (2000) 1011.
[28] A.V. Barzykin, M. Tachiya, J. Phys. Chem. B 110 (2006) 7068.